13

Robust Attenuation of Frequency Varying Disturbances

Kai Zenger and Juha Orivuori
Aalto University School of Electrical Engineering
Finland

1. Introduction

Systems described by differential equations with time-periodic coefficients have a long history in mathematical physics. Applications cover a wide area of systems ranging from helicopter blades, rotor-bearing systems, mechanics of structures, stability of structures influenced by periodic loads, applications in robotics and micro-electromechanical systems etc. (Rao, 2000; Sinha, 2005). Processes characterized by linear time-invariant or time-varying dynamics corrupted by sinusoidal output disturbance belong to this class of systems. Robust and adaptive analysis and synthesis techniques can be used to design suitable controllers, which fulfill the desired disturbance attenuation and other performance characteristics of the closed-loop system.

Despite of the fact that LTP (Linear Time Periodic) system theory has been under research for years (Deskmuhk & Sinha, 2004; Montagnier et al., 2004) the analysis on LTPs with experimental data has been seriously considered only recently (Allen, 2007). The importance of new innovative ideas and products is of utmost importance in modern industrial society. In order to design more accurate and more economical products the importance of model-based control, involving increasingly accurate identification schemes and more effective control methods, have become fully recognized in industrial applications.

An example of the processes related to the topic is vibration control in electrical machines, in which several research groups are currently working. Active vibration control has many applications in various industrial areas, and the need to generate effective but relatively cheap solutions is enormous. The example of electrical machines considered concerns the dampening of rotor vibrations in the so-called critical speed declared by the first flexural rotor bending resonance. In addition, the electromagnetic fields in the air-gap between rotor and stator may couple with the mechanic vibration modes, leading to rotordynamic instability. The vibration caused by this resonance is so considerable that large motors often have to be driven below the critical speed. Smaller motors can be driven also in super-critical speeds, but they have to be accelerated fast over the critical speed. Active vibration control would make it possible to use the motor in its whole operation range freely, according to specified needs given by the load process. Introducing characteristics of this kind for the electric drives of the future would be a major technological break-through, a good example of an innovative technological development.

In practice, the basic electromechanical models of electrical machines can be approximated by linear time-invariant models with a sinusoidal disturbance signal entering at the so-called critical frequency. That frequency can also vary which makes the system model time-variable. The outline of the article is as follows. Two test processes are introduced in Section 2. A systematic and generic model structure valid for these types of systems is presented in Section 3. Three types of controllers for active vibration control are presented in Section 4 and their performance is verified by simulations and practical tests. Specifically the extension to the nonlinear control algorithm presented in Section 4.4 is important, because it extends the optimal controller to a nonlinear one with good robustness properties with respect to variations in rotation frequency. Conclusions are given in Section 5.

2. Problem statement

The control algorithms described in the paper were tested by two test processes to be discussed next.

2.1 An electric machine

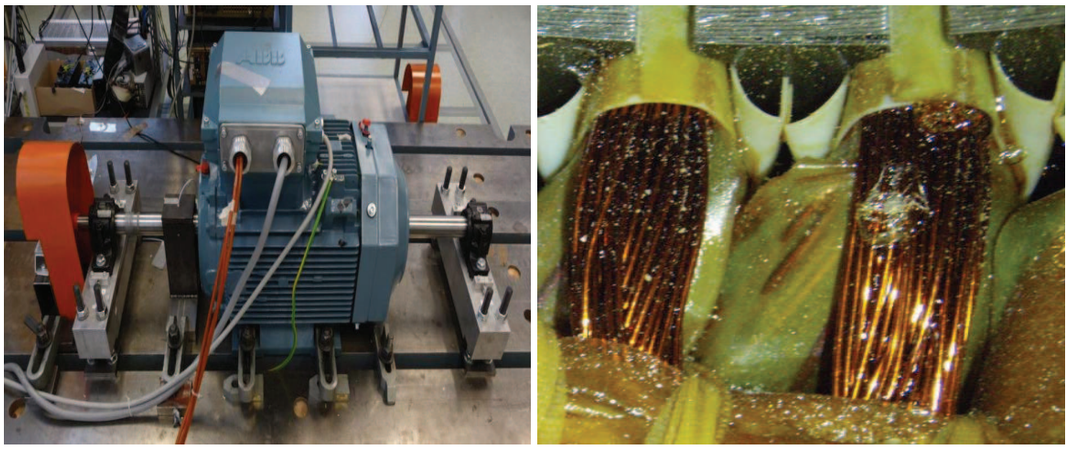

(a) Fig1a (b) Fig1b

Fig. 1. Test machine: A 30 kW three-phase squirrel cage induction motor with an extended rotor shaft (a) and stator windings (b)

In electrical motors both radial and axial vibration modes are of major concern, because they limit the speed at which the motor can be run and also shorten the lifetime of certain parts of the motor. The fundamental vibration forces are typically excited at discrete frequencies (critical frequencies), which depend on the electrodynamics of the rotor and stator (Inman, 2006). In some machines the critical frequency can be passed by accelerating the rotor speed fast beyond it, but specifically in larger machines that is not possible. Hence these machines must be run at subcritical frequencies. It would be a good idea to construct an actuator, which would create a separate magnetic field in the airgap between the stator and rotor. That would cause a counterforce, which would attenuate the vibration mode of the rotor. Running the rotor at critical speeds and beyond will need a stable and robust vibration control system, because at different speeds different vibration modes also wake.

In Fig.1 a 30 kW induction machine is presented, provided with such a new actuator, which is a coil mounted in the stator slots of the machine (b). The electromechanical actuator is an extra winding, which, due to the controlled current, produces the required counter force to damp the rotor vibrations. The actuator is designed such that the interaction with the normal operation of the machine is minimal. More on the design and modelling of the actuator can be found in (Laiho et al., 2008).
Some of the machine parameters are listed in Table 1. The vibration of the rotor is continuously measured in two dimensions and the control algorithm is used to calculate the control current fed into the coil. The schema of the control arrangement is shown in Fig.2. The idea is to

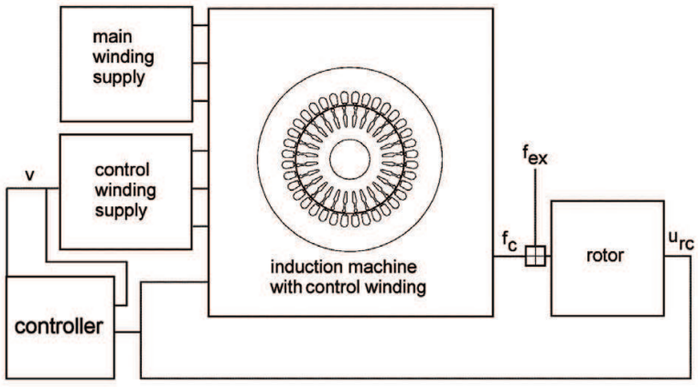

Fig. 2. Rotor vibration control by a built-in new actuator

generate a control force to the rotor through a new actuator consisting of extra windings mounted in the stator slots. An adaptive model-based algorithm controls the currents to the actuator thus generating a magnetic field that induces a force negating the disturbance force exited by the mass imbalance of the rotor. The configuration in the figure includes an excitation force (disturbance) consisting of rotation harmonics and harmonics stemming from the induction machine dynamics. The control force and the disturbance exert a force to the rotor, which results in a rotor center displacement. If the dynamic compensation signal is chosen cleverly, the rotor vibrations can be effectively reduced.
In practical testing the setup shown in Fig.3 has been used. The displacement of the rotor in two dimensions (xy) is measured at one point with displacement transducers, which give a voltage signal proportional to the distance from sensor to the shaft. A digital tachometer at the end of the rotor measures the rotational frequency. The control algorithms were programmed in Matlab/Simulink model and the dSpace interface system and the Real-Time Workshop were used to control the current fed to the actuator winding.

2.2 An industrial rolling process

The second tests were made by a rolling process consisting of a reel, hydraulic actuator and force sensor. The natural frequency of the process was 39 Hz, and the hydraulic actuator acts both as the source of control forces and as a support for the reel. The actuator is connected to the support structures through a force sensor, thus providing information on the forces acting on the reel. The test setup is shown in Fig.4 and the control schema is presented in Fig.5.

Parameter	Value	Unit
supply frequency	50	Hz
rated voltage	400	V
connection	delta	-
rated current	50	A
rated power	30	kW
number of phases	3	-
number of poles	2	-
rated slip	1	%
rotor mass	55.8	kg
rotor shaft length	1560	mm
critical speed	37.5	Hz
width of the air-gap	1	mm

Table 1. Main parameters of the test motor

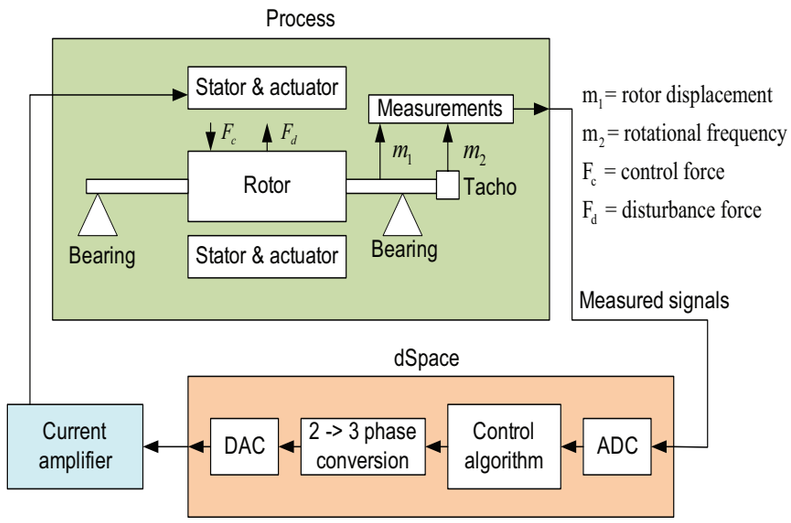

Fig. 3. Schema of the test setup (motor)

3. Modeling and identification

Starting from the first principles of electromagnetics (Chiasson, 2005; Fuller et al., 1995) and structure mechanics, the vibration model can for a two-pole cage induction machine be written in the form (Laiho et al., 2008)

$$\begin{aligned} \dot{q} &= Aq + Bv + Gf_{ex} \\ u_{rc} &= Cq \end{aligned} \tag{1}$$

where q denotes the states (real and complex) of the system, v is the control signal of the actuator, f_{ex} is the sinusoidal disturbance causing the vibration at the critical frequency, and u_{rc} is the radial rotor movement in two dimensions. The matrices A, B, G and C are constant. The constant parameter values can be identified by the well-known methods (Holopainen et al., 2004; Laiho et al., 2008; Repo & Arkkio, 2006). The results obtained

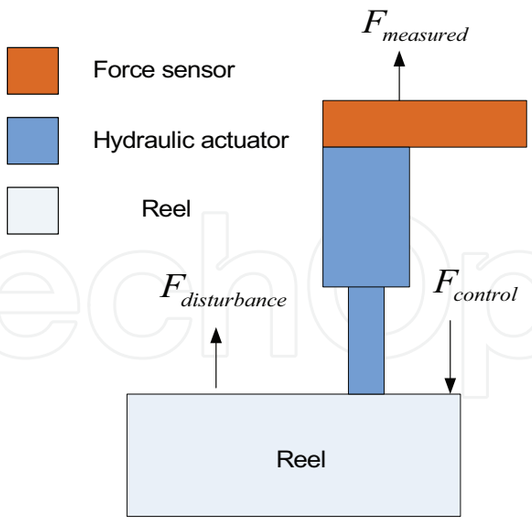

Fig. 4. The test setup (industrial rolling process)

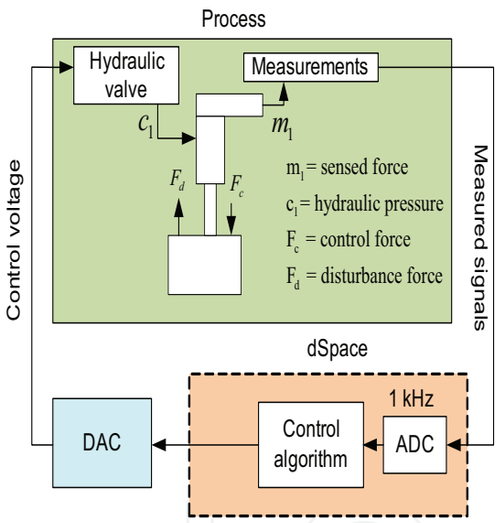

Fig. 5. The controller schema

by using finite-element (FE) model as the "real" process have been good and accurate (Laiho et al., 2007), when both prediction error method (PEM) and subspace identification (SUB) have been used. Since the running speed of the motor was considered to be below 60 Hz, the sampling rate was chosen to be 1 kHz. A 12th order state-space model was used as the model structure (four inputs and two outputs corresponding to the control voltages, rotor displacements and produced control forces in two dimensions). The model order was chosen based on the frequency response calculated from the measurement data, from which the approximate number of poles and zeros were estimated.

In identification a pseudo random (PSR) control signal was used in control inputs. That excites rotor dynamics on a wide frequency range, which in limited only by the sampling rate. However, because the second control input corresponds to the rotor position and has a big influence on the produced force a pure white noise signal cannot be used here. Therefore

the model output of the rotor position added with a small PSR signal to prevent correlation was used as the second control input. After identification the model was validated by using independent validation data. The fit was larger than 80 per cent, which was considered to be adequate for control purposes. The results have later been confirmed by tests carried out by using the real test machine data, and the results were found to be equally good.
The model structure is then as shown in Fig.6, where the actuator model and electromechanic model of the rotor have been separated, and the sinusoidal disturbance term is used to model the force that causes the radial vibration of the rotor. In Fig.6a the models of the actuator and rotor have been separated and the disturbance is modelled to enter at the input of the rotor model. The internal feedback shown is caused by the unbalanced magnetic pull (UMP), which means that the rotor when moved from the center position in the airgap causes an extra distortion in the magnetic field. That causes an extra force, which can be taken into consideration in the actuator model. However, in practical tests it is impossible to separate the models of the actuator and rotor dynamics, and therefore the model in Fig.6b has been used in identification. Because the models are approximated by linear dynamics, the sinusoidal disturbance signal can be moved to the process output, and the actuator and rotor models can be combined.
In Fig. 6a the 4-state dynamical (Jeffcott) model for the radial rotor dynamics is

$$\begin{aligned} \dot{x}_r(t) &= A_r x(t) + B_r u_r(t) \\ y_r(t) &= C_r x(t) \end{aligned} \tag{2}$$

where y_r is the 2-dimensional rotor displacement from the center axis in xy-coordinates, and u_r is the sum of the actuator and disturbance forces. The actuator model is

$$\begin{aligned} \dot{x}_a(t) &= A_a x_a(t) + \begin{bmatrix} B_{a1} & B_{a2} \end{bmatrix} \begin{bmatrix} y_r(t) \\ u(t) \end{bmatrix} \\ y_a(t) &= C_a x_a(t) \end{aligned} \tag{3}$$

where y_a are the forces generated by the actuator, and u are the control voltages fed into the windings. The self-excited sinusoidal disturbance signal is generated by (given here in two dimensions)

$$\begin{aligned} \dot{x}_d(t) = A_d x_d(t) &= \begin{bmatrix} 0 & 1 & 0 & 0 \\ -\omega_d^2 & 0 & 0 & 0 \\ 0 & 0 & 0 & 1 \\ 0 & 0 & -\omega_d^2 & 0 \end{bmatrix} x_d(t) \\ d(t) = C_d x_d(t) &= \begin{bmatrix} 1 & 0 & 0 & 0 \\ 0 & 0 & 1 & 0 \end{bmatrix} x_d(t) \end{aligned} \tag{4}$$

where ω_d is the angular frequency of the disturbance and $d(t)$ denotes the disturbance forces in xy-directions. The initial values of the state are chosen such that the disturbance consists of two sinusoidal signals with 90 degree phase shift (sine and cosine waves). The initial values are then

$$x_d(0) = \begin{bmatrix} x_{\sin}(0) \\ x_{\cos}(0) \end{bmatrix} = \begin{bmatrix} 0 \\ A\omega_d \\ A \\ 0 \end{bmatrix}$$

where A is the amplitude of the disturbance. The models of the actuator, rotor and disturbance can be combined into one state-space representation

$$\begin{aligned} \dot{x}_p(t) &= A_p x_p(t) + B_p u(t) = \begin{bmatrix} A_r & B_r C_a & B_r C_d \\ B_{a1} C_r & A_a & 0 \\ 0 & 0 & A_d \end{bmatrix} x_p(t) + \begin{bmatrix} 0 \\ B_{a2} \\ 0 \end{bmatrix} u(t) \\ y_r(t) &= C_p x_p(t) = \begin{bmatrix} C_r & 0 & 0 \end{bmatrix} x_p(t) \end{aligned} \tag{5}$$

with

$$x_p = \begin{bmatrix} x_r \\ x_a \\ x_d \end{bmatrix}$$

As mentioned, the actuator and rotor model can be combined and the disturbance can be moved to enter at the output of the process (according to Fig. 6b). The state-space representation of the actuator-rotor model is then

$$\begin{aligned} \dot{x}_{ar}(t) &= A_{ar} x_{ar}(t) + B_{ar} u(t) \\ y_{ar}(t) &= C_{ar} x_{ar}(t) \end{aligned} \tag{6}$$

where u is a vector of applied control voltages and y_{ar} is vector of rotor displacements. The whole system can be modeled as

$$\begin{aligned} \dot{x}_p(t) &= A_p x_p(t) + B_p u_p(t) = \begin{bmatrix} A_{ar} & 0 \\ 0 & A_d \end{bmatrix} x_p(t) + \begin{bmatrix} B_{ar} \\ 0 \end{bmatrix} u(t) \\ y_r(t) &= C_p x_p(t) = \begin{bmatrix} C_{ar} & C_d \end{bmatrix} x_p(t) \end{aligned} \tag{7}$$

with

$$x_p(t) = \begin{bmatrix} x_{ar}(t) \\ x_d(t) \end{bmatrix}$$

The process was identified with a sampling frequency of 1 kHz, which was considered adequate since the running speed of the motor was about 60 Hz and therefore well below 100 Hz. Pseudorandom signals were used as control forces in both channels separately, and the prediction error method (PEM) was used (Ljung, 1999) to identify a 12th order state-space representation of the system.
The identified process model is compared to real process data, and the results are shown in Figs.7 and 8, respectively. The fit in x and y directions were calculated as 72.5 % and 80.08 %, which is considered to be appropriate. From the frequency domain result it is seen that for lower frequency the model agrees well with response obtained form measured data, but in higher frequencies there is a clear difference. That is because the physical model used behind the identification is only valid up to a certain frequency, and above that there exist unmodelled dynamics.

4. Control design

In the following sections different control methods are presented for vibration control of single or multiple disturbances with a constant or varying disturbance frequencies. Two of the methods are based on the *linear quadratic gaussian* (LQ) control, and one belongs to the class of *higher harmonic control* algorithms (HHC), which is also known as *convergent control*. If the

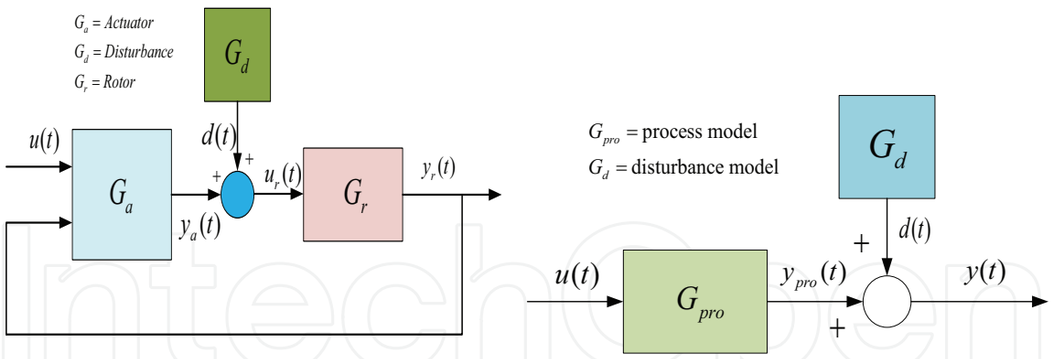

(a) Fig6a (b) Fig6b

Fig. 6. Process models for the actuator, rotor and sinusoidal disturbance

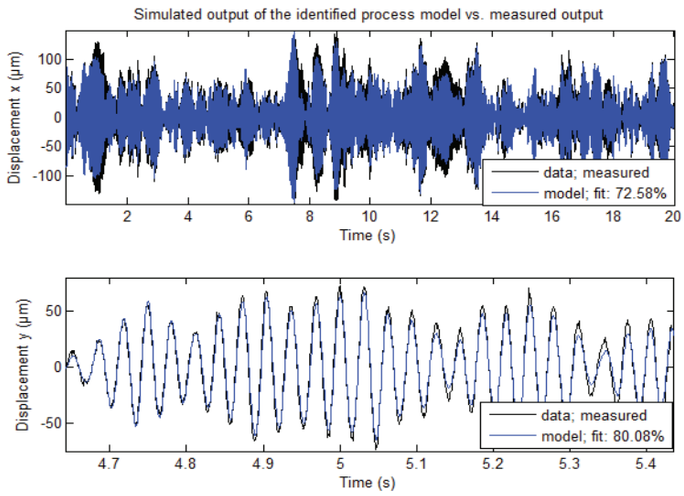

Fig. 7. Validation of the actuator-rotor model in time domain

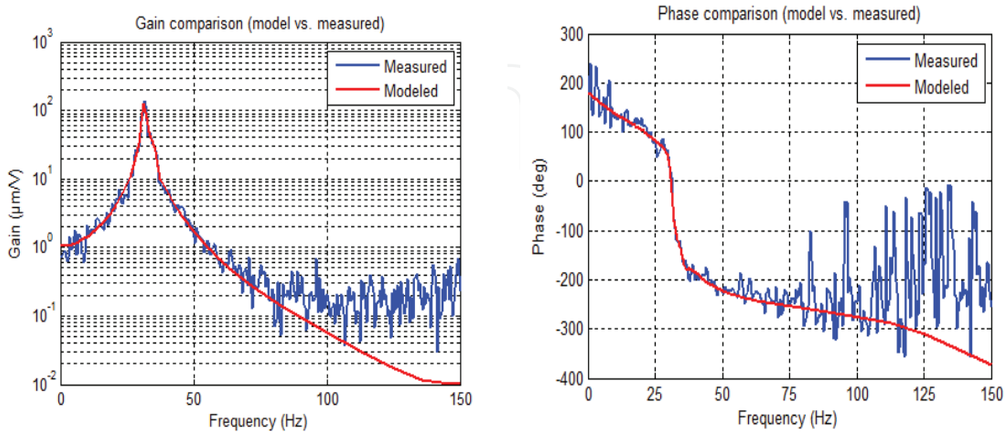

Fig. 8. Validation of the actuator-rotor model in frequency domain

sinusoidal disturbance frequency signal varies in frequency, the algorithms must be modified by combining them and using direct frequency measurement or frequency tracking.

4.1 Direct optimal feedback design

In this method the suppressing of tonal disturbance is posed as a dynamic optimization problem, which can be solved by the well-known LQ theory. The idea is again that the model generating the disturbance is embedded in the process model, and that information is then automatically used when minimizing the design criterion. That leads to a control algorithm which inputs a signal of the same amplitude but opposite phase to the system thus canceling the disturbance. The problem can be defined in several scenarios, e.g. the disturbance can be modelled to enter at the process input or output, the signal to be minimized can vary etc. Starting from the generic model

$$\begin{aligned} \dot{x}(t) &= Ax(t) + Bu(t) = \begin{bmatrix} A_p & 0 \\ 0 & A_d \end{bmatrix} x(t) + \begin{bmatrix} B_p \\ 0 \end{bmatrix} u(t) \\ y(t) &= \begin{bmatrix} C_p & C_d \end{bmatrix} x(t) \end{aligned} \tag{8}$$

the control criterion is set

$$J = \int_0^\infty \left(z^T(\tau) Q z(\tau) + u^T(\tau) R u(\tau) \right) d\tau \tag{9}$$

where z is a freely chosen performance variable and $Q \geq 0$, $R > 0$ are the weighing matrices for the performance variable and control effort. By inserting $z(t) = C_z x(t)$ the criterion changes into the standard LQ form

$$J = \int_0^\infty \left(x^T(\tau) C_z^T Q C_z x(\tau) + u^T(\tau) R u(\tau) \right) d\tau \tag{10}$$

The disturbance dynamics can be modelled as

$$\begin{aligned} \dot{x}_d(t) &= A_d x_d(t) = \begin{bmatrix} A_{d1} & \cdots & 0 & 0 \\ \vdots & \ddots & \vdots & \vdots \\ 0 & \cdots & A_{dn} & 0 \\ 0 & \cdots & 0 & -\epsilon \end{bmatrix} x_{dn}(t) \\ d(t) &= C_d x_d(t) = \begin{bmatrix} C_{d1} & \cdots & C_{dn} & 0 \end{bmatrix} x_{dn}(t) \end{aligned} \tag{11}$$

where

$$A_{dn} = \begin{bmatrix} 0 & 1 \\ -\omega_{dn}^2 & -\varepsilon \end{bmatrix}, \quad i = 1, 2, ..., n$$

and the initial values

$$x(0) = \begin{bmatrix} x_{d1}^T(0) & \cdots & x_{dn}^T(0) & b \end{bmatrix}^T$$

According to the formalism a sum of n sinusoidal disturbance components (angular frequencies ω_{dn}) enter the system. The very small number ϵ is added in order the augmented system to be stabilizable, which is needed for the solution to exist. The damping of the resulting sinusoidal is so low that it does not affect the practical use of the optimal controller.

The constant b can be used for a constant bias term in the disturbance. Compare the disturbance modelling also to that presented in equations (4) and (5).
To minimize of sinusoidal disturbances the following performance variable can be chosen

$$z(t) = \left[C_p \vdots \left[C_{d1} \cdots C_{dn} \; 0 \right] \right] x(t) = \left[C_p \vdots C_d \right] x(t) = C_z x(t) \tag{12}$$

which leads to the cost function (10)
The solution of the LQ problem can now be obtained by standard techniques (Anderson & Moore, 1989) as

$$u(t) = -Lx(t) = -R^{-1} B^T S x(t) \tag{13}$$

where S is the solution of the algebraic Riccati equation

$$A^T S + SA - SBR^{-1} B^T S + Q = 0 \tag{14}$$

It is also possible to choose simply $z(t) = x(t)$ in (9). To force the states approach zero it is in this case necessary to introduce augmented states

$$x_{aug}(t) = \int_0^t \left(y_{ar}(\tau) + d(\tau) \right) d\tau = \left[C_{ar} \; C_d \right] \int_0^t \left(\left[x_{ar}(\tau)^T \; x_d(\tau)^T \right]^T \right) d\tau \tag{15}$$

The system to which the LQ design is used is then

$$\begin{aligned} \dot{x}(t) &= \begin{bmatrix} \dot{x}_p(t) \\ \dot{x}_{aug}(t) \end{bmatrix} = \underbrace{\begin{bmatrix} A_p & \vdots & 0 \\ \cdots & \vdots & \cdots \\ \left[C_{ar} \; C_d \right] & \vdots & 0 \end{bmatrix}}_{A_{aug}} x(t) + \underbrace{\begin{bmatrix} B_p \\ \cdots \\ 0 \end{bmatrix}}_{B_{aug}} u(t) \\ y_r(t) &= \underbrace{\left[C_p \; 0 \right]}_{C_{aug}} x(t) \end{aligned} \tag{16}$$

In this design the weights in Q corresponding to the augmented states should be set to considerably high values, e.g. values like 10^5 have been used.
Usually a state observer must be used to implement the control law. For example, in the configuration shown in Fig.6a (see also equation (5)) that has the form

$$\begin{aligned} \dot{\hat{x}}(t) &= A_p \hat{x}(t) + B_p u(t) + K \left(y_r(t) - \hat{y}_r(t) \right) \\ y_{obs} &= \hat{x}(t) \end{aligned} \tag{17}$$

The gain in the estimator can be chosen based on the duality between the LQ optimal controller and the estimator. The state error dynamics $\tilde{x}(t) = x(t) - \hat{x}(t)$ follows the dynamics

$$\dot{\tilde{x}}(t) = \left(A_p - KC_p \right) \tilde{x}(t) \tag{18}$$

which is similar to

$$\dot{x}_N(t) = A_N x_N(t) + B_N u_N(t) \tag{19}$$

with $A_N = A_p^T, B_N = C_p^T, K_N = K^T$ and $u_N(t) = -K_N x_N(t)$. The weighting matrix K_N can be determined by minimizing

$$J_{obs} = \int_0^\infty \left(x_N(t)^T Q_{obs} x_N(t) + u_N(t)^T R_{obs} u_N(t) \right) dt \tag{20}$$

where the matrices Q_{obs} and R_{obs} contain the weights for the relative state estimation error and its convergence rate.
The optimal control law (13) can now be combined with the observer model (17). Including the augmented states (15) the control law can be stated as

$$\begin{aligned} \dot{x}_{\mathrm{LQ}}(t) &= \begin{bmatrix} \dot{\hat{x}}(t) \\ \dot{\hat{x}}_{\mathrm{aug}}(t) \end{bmatrix} = \underbrace{\left(\begin{bmatrix} A_p - KC_p & 0 \\ C_p & 0 \end{bmatrix} - \begin{bmatrix} B_p \\ 0 \end{bmatrix} L \right)}_{A_{\mathrm{LQ}}} x_{\mathrm{LQ}}(t) + \underbrace{\begin{bmatrix} K \\ 0 \end{bmatrix}}_{B_{\mathrm{LQ}}} y_r(t) \\ u_{\mathrm{LQ}}(t) &= \underbrace{-L}_{C_{\mathrm{LQ}}} x_{\mathrm{LQ}}(t) \end{aligned} \tag{21}$$

where y_r is the rotor displacement, u_{LQ} is the optimal control signal, and A_{LQ}, B_{LQ} and C_{LQ} are the parameters of the controller.

4.2 Convergent controller

The convergent control (CC) algorithm (also known as instantaneous harmonic control (IHC) is a feedforward control method to compensate a disturbance at a certain frequency (Daley et al., 2008). It is somewhat similar to the well-known least means squares compensator (LMS), (Fuller et al., 1995; Knospe et al., 1994) which has traditionally been used in many frequency compensating methods in signal processing. A basic schema is presented in Fig.9. The term r is a periodic signal of the same frequency as d, but possibly with a different

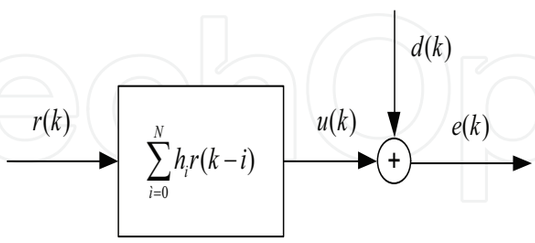

Fig. 9. Feedforward compensation of a disturbance signal

amplitude and phase. The idea is to change the filter parameters h_i such that the signal u compensates the disturbance d. The standard LMS algorithm that minimizes the squared error can be derived to be as

$$h_i(k+1) = h_i(k) - \alpha r(k-i) e(k) \tag{22}$$

where α is a tuning parameter (Fuller et al., 1995; Tammi, 2007). In the CC algorithm the process dynamics is presented by means of the Fourier coefficients as

$$E_F(k) = G_F U_F(k) + D_F(k) \tag{23}$$

where G_F is the complex frequency response of the system and the symbols E_F, U_F and D_F are the Fourier coefficients of the error, control and disturbance signals. For example

$$E_F^{\omega_n} = \frac{1}{N}\sum_{k=0}^{N-1} e(k)e^{-2i\pi kn/N} \approx e(k)e^{-i\omega_n t}$$

where N is the number of samples in one signal period, and n is the number of the spectral line of the corresponding frequency. If the sampling time is T_s, then $t = kT_s$.
The criterion to be minimized is $J = E_F^* E_F$ which gives

$$U_F = -\left(G_F^* G_F\right)^{-1} G_F^* D_F = -A_F D_F \tag{24}$$

where * denotes the complex transpose. The pseudoinverse is used if necessary when calculating the inverse matrix. In terms of Fourier coefficients the Convergent Control Algorithm can be written as

$$U_F(k+1) = \beta U_F(k) - \alpha A_F E_F(k) \tag{25}$$

where α and β are tuning parameters. It can be shown (Daley et al., 2008; Tammi, 2007) that the control algorithm can be presented in the form of a linear time-invariant pulse transfer function

$$G_{cc}(z) = \frac{U(z)}{Y(z)} = \beta \frac{\mathrm{Re}\left(G_F\left(e^{i\omega_k}\right)^{-1}\right) z^2 - \alpha \mathrm{Re}\left(G_F\left(e^{i\omega_k}\right)^{-1} e^{-i\omega_k T_s}\right) z}{z^2 - 2\alpha\cos\left(\omega_k T_s\right) z + \alpha^2} \tag{26}$$

where $Y(z)$ is the sampled plant output and $U(z)$ is the sampled control signal.
The convergent controller can operate like an LMS controller in series with the plant, by using a reference signal r proportional to the disturbance signal to be compensated. The 'plant' can here mean also the process controlled by a wide-frequency band controller like the LQ controller for instance.

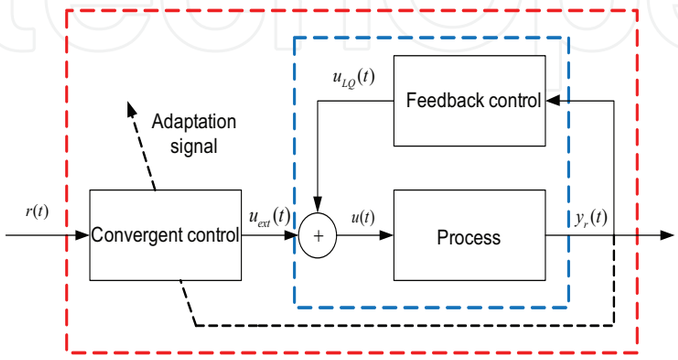

Fig. 10. Convergent controller in series with a controlled plant

Alternatively, the CC controller can be connected in parallel with the LQ-controller, then having the plant output as the input signal. Several CC controllers (tuned for different frequencies) can also be connected in parallel in this configuration, see Fig.11.

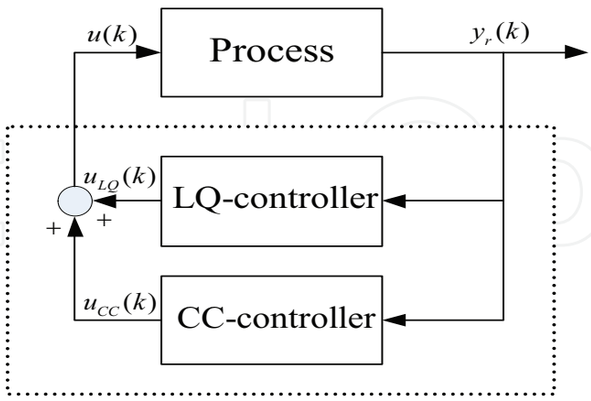

Fig. 11. Convergent controller connected in parallel with the LQ controller

4.3 Simulations and test runs

The controller performance was tested in two phases. Firstly, extensive simulations by using a finite element (FE) model of the electrical machine and actuator were carried out. Secondly, the control algorithms were implemented in the test machine discussed in Section 2.1 by using a dSpace system as the program-machine interface. The disturbance frequency was 49.5 Hz, and the controller was discretized with the sampling frequency 1 kHz. Time domain simulations are shown in Figs. 12 and 13. The damping is observed to be about 97 per cent, which is a good result.

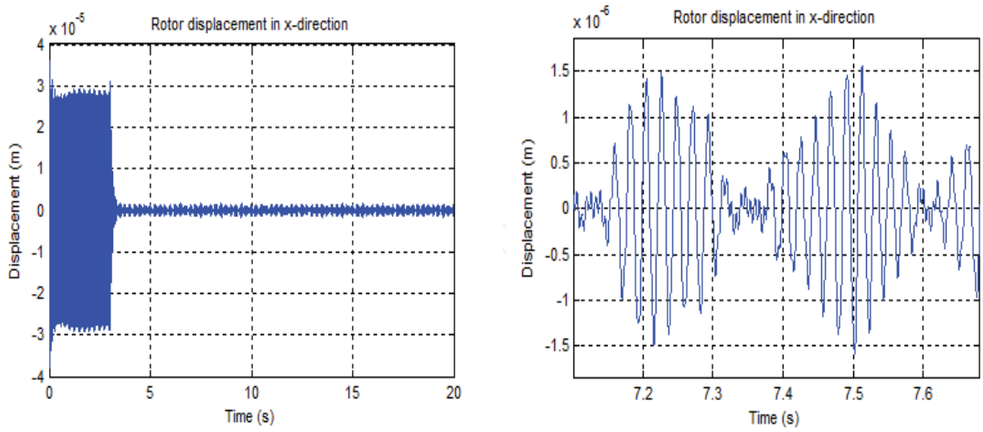

Fig. 12. Simulation result in time domain (rotor vibration in x-direction)

The critical frequency of the 30 kW test motor was 37.7 Hz. However, due to vibrations the rotor could not be driven at this speed in open loop, and both the identification and initial control tests were performed at 32 Hz rotation frequency. In the control tests the LQ controller was used alone first, after which the CC controller was connected, in order to verify the performance of these two control configurations. Both controllers were discretized at 5 kHz sampling rate.

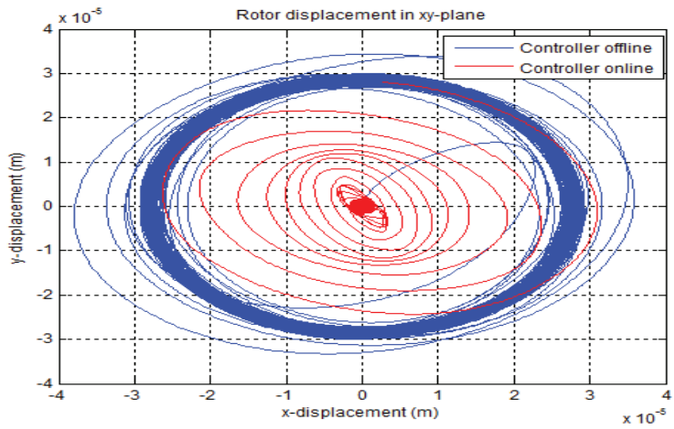

Fig. 13. Simulated rotor vibration in xy-plot

The test results are shown in Figs. 14-17. In Fig.14 the control signal and rotor vibration amplitude are shown, when the machine was driven at 32.5 Hz. The LQ controller was used first alone, and then the CC controller was connected. It is seen that the CC controller improves the performance somewhat, and generally the vibration damping is good and well comparable to the results obtained by simulations. The same can be noticed from the xy-plot shown in Fig.15.

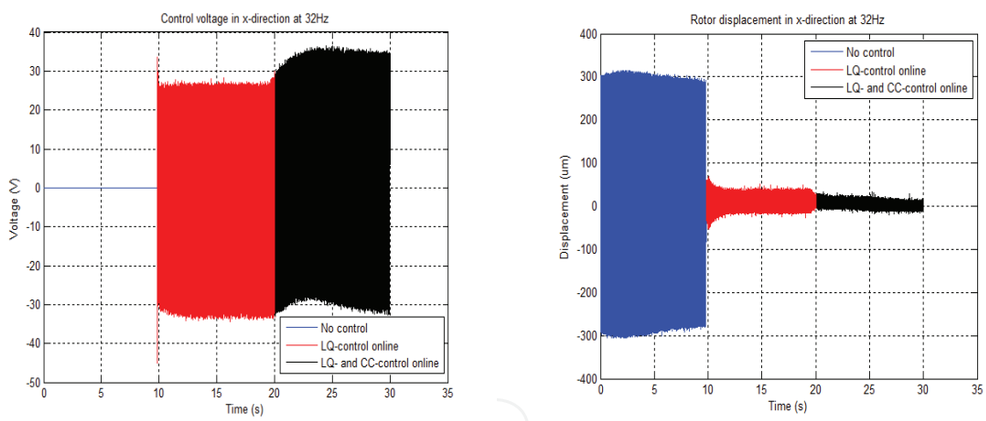

Fig. 14. Test machine runs at 32 Hz speed: Control voltage and rotor displacement in x-direction

Next, the operation speed was increased to the critical frequency 37.5 Hz. Controller(s) tuned for this frequency could be driven without any problems at this speed. Similar results as above are shown in Figs.16 and 17. It is remarkable that now connecting the CC controller on improved the results more than before. So far there is no clear explanation to this behaviour.

4.4 Nonlinear controller

If the frequency of the disturbance signal is varying, the performance of a controller with constant coefficients deteriorates considerably. An immediate solution to the problem involves the use of continuous gain scheduling, in which the controller coefficients are modified according to the current disturbance frequency. To this end the disturbance

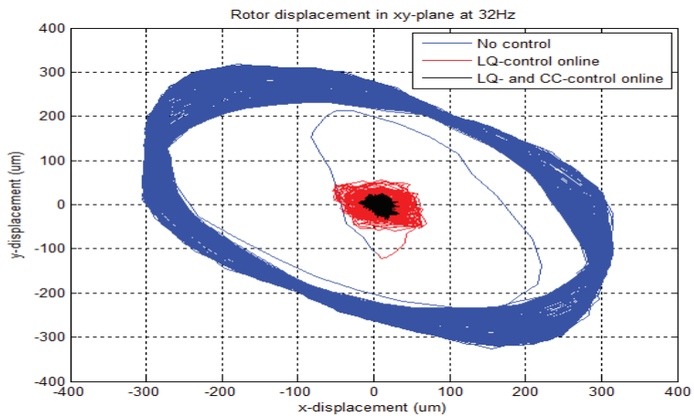

Fig. 15. Test machine runs at 32 Hz speed: xy-plot

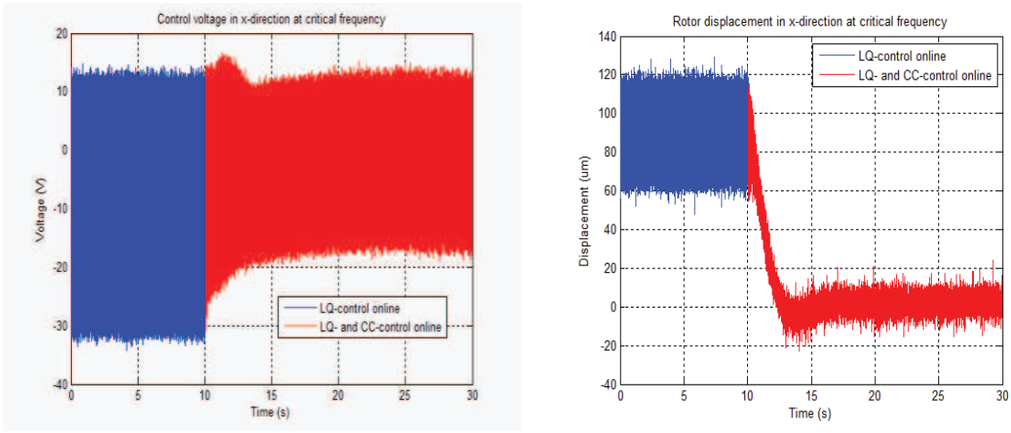

Fig. 16. Test machine runs at 37.5 Hz critical speed: Control voltage and rotor displacement in x-direction

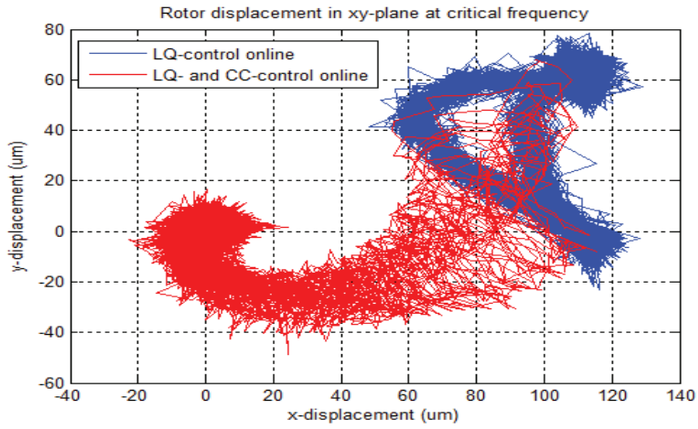

Fig. 17. Test machine runs at 37.5 Hz critical speed: xy-plot

frequency (usually the rotating frequency) has to be measured of tracked (Orivuori & Zenger, 2010; Orivuori et al., 2010). The state estimator can be written in the form

$$\dot{\hat{x}}(t,\omega_{hz}) = \left(A\left(\omega_{hz}\right) - K\left(\omega_{hz}\right)C\right)\hat{x}(t,\omega_{hz}) + Bu(t) + K(\omega_{hz})y(t) \tag{27}$$

where it has been assumed that the model topology is as in Fig.6b and the disturbance model is included in the system matrix A. The matrix K changes as a function of frequency as

$$K(\omega_{hz}) = \left[\, f_1(\omega_{hz})\ f_2(\omega_{hz})\ \cdots\ f_n(\omega_{hz}) \,\right]^T \tag{28}$$

where f_i are suitable functions of frequency. Solving the linear optimal control problem in a frequency grid gives the values of K, which can be presented like in Fig.18 The functions f_i

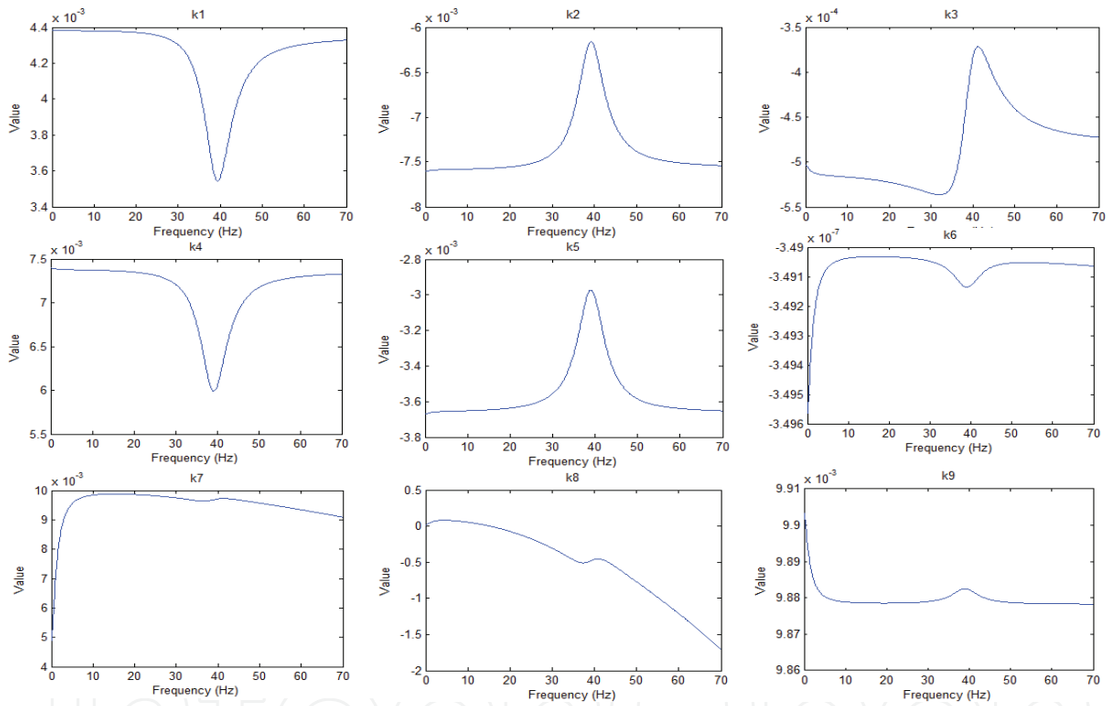

Fig. 18. Projections of the hypersurface to the elements of K

can be chosen to be polynomials, so that the feedback gain has the form

$$K(\omega_{hz}) = \begin{bmatrix} a_{11} & a_{12} & \cdots & a_{1m} \\ a_{21} & a_{22} & \cdots & a_{2m} \\ \vdots & \vdots & \ddots & \vdots \\ a_{n1} & a_{n2} & \cdots & a_{nm} \end{bmatrix} u_{\omega}(\omega_{hz}) \tag{29}$$

where a_{ij} are the polynomial coefficients and

$$u_\omega(\omega_{hz}) = \left[\omega_{hz}^{m-1} \cdots \omega_{hz}^2 \ \omega_{hz} \ 1 \right]^T \tag{30}$$

The optimal control gain $L(\omega_{hz})$ can be computed similarly.
The controller was tested with the industrial rolling process presented in Section 2.2. A sinusoidal sweep disturbance signal was used, which corresponds to a varying rotational speed of the reel with constant width. The rotation frequency ranged over the frequency range 5 Hz..50 Hz. Before the practical tests the theoretical performance of the controller was analyzed. The result is shown in Fig.19, which shows a neat damping of the vibration near the critical frequency 39 Hz. Simulation and practical test results are shown in Figs.20 and

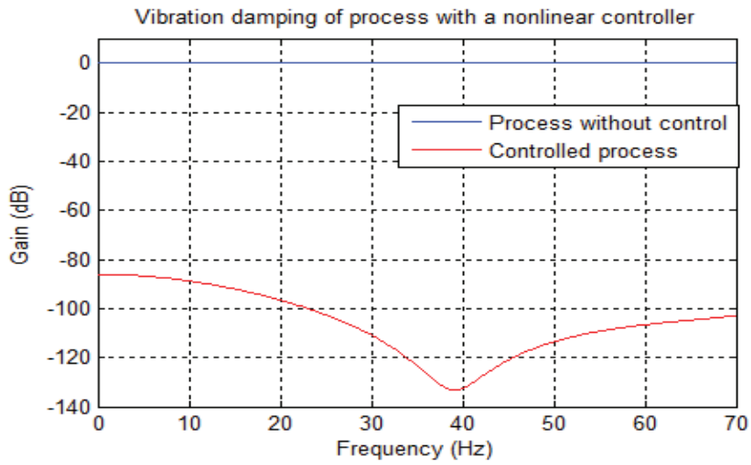

Fig. 19. Theoretical damping achieved with the nonlinear controller

21, respectively. The controller turns out to be effective over the whole frequency range the damping ratio being 99 per cent in simulation and about 90 per cent in practical tests. The result of the good performance of the nonlinear controller is further verified by the output spectrum of the process obtained with and without control. The result is shown in Fig.22.

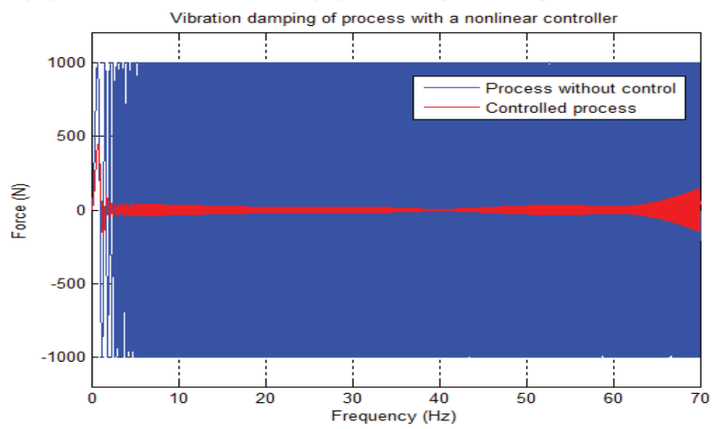

Fig. 20. Simulated performance of the nonlinear controller

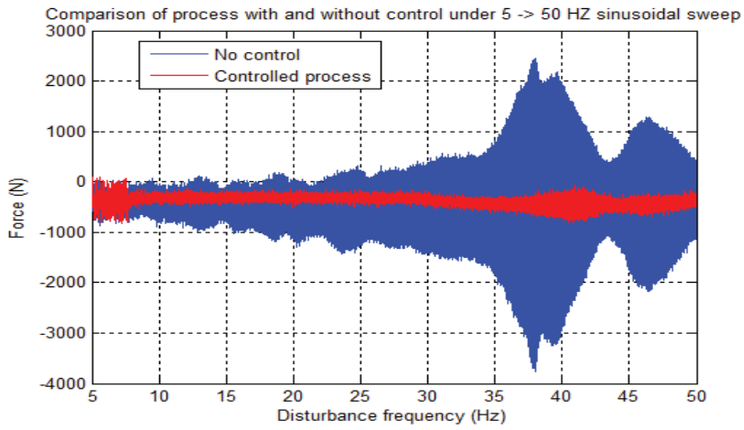

Fig. 21. Real performance of the nonlinear controller

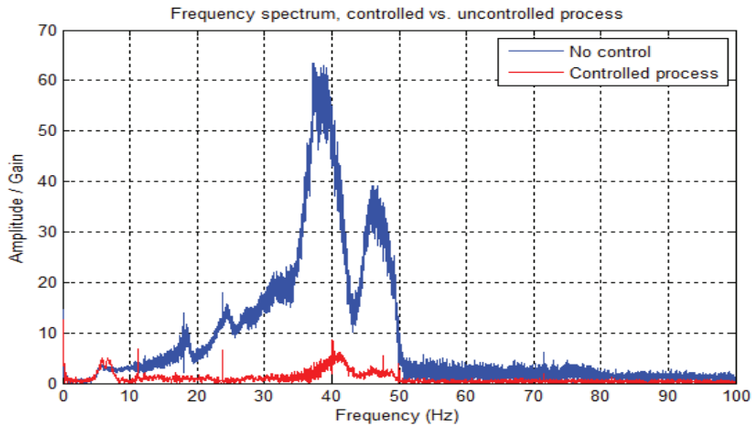

Fig. 22. Frequency spectra of the process output with and without control

5. Conclusion

Vibration control in rotating machinery is an important topic of research both from theoretical and practical viewpoints. Generic methods which are suitable for a large class of such processes are needed in order to make the analysis and controller design transparent and straightforward. LQ control theory offers a good and easy to learn model-based control technique, which is effective and easily implemented for industrial processes. The control algorithm can be extended to the nonlinear case covering systems with varying disturbance frequencies. The performance of such an algorithm has been studied in the paper, and the performance has been verified by analysis, simulation and practical tests of two different processes. The vibration control results have been excellent. In future research it is investigated, how the developed methods can be modified to be used is semi-active vibration control. That is important, because active control has its risks, and all industrial users are not willing to use active control methods.

6. Acknowledgement

The research has been supported by TEKES (The Finnish Funding Agency for Technology and Innovation) and the Academy of Finland.

7. References

Allen, M. S. (2007). Floquet Experimental Modal Analysis for System Identification of Linear Time-Periodic Systems, In: *Proceedings of the ASME 2007, IDETC/CIE*, 11 pages, September 2007, Las Vegas, Nevada, USA.

Anderson, B. D. O. & Moore, J. B. (1989). *Optimal Control: Linear Quadratic Methods*, Prentice-Hall, Englewood Cliffs, NJ.

Chiasson, J. N. (2005). *Modeling and High Performance Control of Electric Machines*, John Wiley, IEEE, Hoboken, NJ.

Daley, S.; Zazas, I.; Hätönen, J. (2008). Harmonic Control of a 'Smart Spring' Machinery Vibration Isolation System, In: *Proceedings of the Institution of Mechanical Engineers, Part M: Journal of Engineering for the Maritime Environment*, Vol. 22, No. 2, pp. 109–119.

Deskmuhk, V. S & Sinha, S. C. (2004). Control of Dynamical Systems with Time-Periodic Coefficients via the Lyapunov-Floquet Transformation and Backstepping Technique, *Journal of Vibration and Control*, Vol. 10, 2004, pp. 1517–1533.

Fuller, C. R.; Elliott, S. J.; Nelson, P. A. (1995). *Active Control of Vibration*, Academic Press, London.

Gupta, N. K. (1980). Frequency-shaped cost functionals: Extension of linear-quadratic-Gaussian design methods, *Journal of Guidance and Control*, Vol. 3, No. 6, 1980, pp. 529–535.

Holopainen, T. P.; Tenhunen, A.; Lantto, E.; Arkkio, A. (2004). Numerical Identification of Electromechanic Force Parameters for Linearized Rotordynamic Model of Cage Induction Motors, *Journal of Vibration and Acoustics*, Vol. 126, No. 3, 2004, pp. 384–390.

Inman, D. J. (2006). *Vibration With Control*, Wiley, Hoboken, NJ.

Knospe, C. R.; Hope, R. W.; Fedigan, S. J.; Williams, R. D. (1994). New Results in the Control of Rotor Synchronous Vibration. In: *Proceedings of the Fourth International Symposium on Magnetic Bearings*, Hochschulverlag AG, Zurich, Switzerland.

Laiho, A.; Holopainen, T. P.; Klinge, P.; Arkkio, A. (2007). Distributed Model For Electromechanical Interaction in Rotordynamics of Cage Rotor Electrical Machines, *Journal of Sound and Vibration*, Vol. 302, Issues 4-5, 2007, pp. 683–698.

Laiho, A.; Tammi, K.; Zenger, K.; Arkkio, A. (2008). A Model-Based Flexural Rotor Vibration Control in Cage Induction Electrical Machines by a Built-In Force Actuator, *Electrical Engineering (Archiv fűr Elektrotechnik)*, Vol. 90, No. 6, 2008, pp. 407–423.

Ljung, L. (1999). *System Identification: Theory for the User*, 2nd Ed., Prentice Hall, Upper Saddle River, NJ.

Montagnier, P.; Spiteri, R. J.; Angeles, J. (2004). The Control of Linear Time-Periodic Systems Using Floquet-Lyapunov Theory, *International Journal of Control*, Vol. 77, No. 20, March 2004, pp. 472–490.

Orivuori, J. & Zenger, K. (2010). Active Control of Vibrations in a Rolling Process by Nonlinear Optimal Controller, In: *Proceedings of the 10th International Conference on Motion and Vibration Control (Movic 2010)*, August 2010, Tokyo, Japan.

Orivuori, J.; Zazas, I.; Daley, S. (2010). Active Control of a Frequency Varying Tonal Disturbance by Nonlinear Optimal Controller with Frequency Tracking, In: *Proceedings of the IFAC Workshop of Periodic Control Systems (Psyco 2010)*, August 2010, Antalya, Turkey.

Rao, J. D. (2000). *Vibratory Condition Monitoring of Machines*, Narosa Publishing House, New Delhi, India.

Repo, A-K. & Arkkio, A. (2006). Numerical Impulse Response Test to Estimate Circuit-Model Parameters for Induction Machines, *IEE Proceedings, Electric Power Applications*, Vol. 153, No. 6, 2006, pp. 883–890.

Sinha, S. C. (2005). Analysis and Control of Nonlinear Dynamical Systems with Periodic Coefficients, In: *Proceedings of the Workshop on Nonlinear Phenomena, Modeling and their applications*, SP-Brazil, Eds. JM Balthazar, RMLRF Brasil, EEN Macau, B. R. Pontes and L C S Goes, 2-4 May, 2005.

Tammi, K. (2007). *Active Control of Rotor Vibrations - Identification, Feedback, Feedforward and Repetitive Control Methods*, Doctoral thesis, VTT Publications 634, Espoo: Otamedia.

Sievers, L. A.; Blackwood, G. H.; Mercadal, M.; von Flotow, A. H. (1991). MIMO Narrowband Disturbance Rejection Using Frequency Shaping of Cost Functionals, In: *Proceedings of American Control Conference*, Boston, MA, USA.

Recent Advances in Robust Control - Novel Approaches and Design Methods

Edited by Dr. Andreas Mueller

ISBN 978-953-307-339-2
Hard cover, 462 pages
Publisher InTech
Published online 07, November, 2011
Published in print edition November, 2011

Robust control has been a topic of active research in the last three decades culminating in H_2/H_\infty and \mu design methods followed by research on parametric robustness, initially motivated by Kharitonov's theorem, the extension to non-linear time delay systems, and other more recent methods. The two volumes of Recent Advances in Robust Control give a selective overview of recent theoretical developments and present selected application examples. The volumes comprise 39 contributions covering various theoretical aspects as well as different application areas. The first volume covers selected problems in the theory of robust control and its application to robotic and electromechanical systems. The second volume is dedicated to special topics in robust control and problem specific solutions. Recent Advances in Robust Control will be a valuable reference for those interested in the recent theoretical advances and for researchers working in the broad field of robotics and mechatronics.

How to reference

In order to correctly reference this scholarly work, feel free to copy and paste the following:

Kai Zenger and Juha Orivuori (2011). Robust Attenuation of Frequency Varying Disturbances, Recent Advances in Robust Control - Novel Approaches and Design Methods, Dr. Andreas Mueller (Ed.), ISBN: 978-953-307-339-2, InTech, Available from: http://www.intechopen.com/books/recent-advances-in-robust-control-novel-approaches-and-design-methods/robust-attenuation-of-frequency-varying-disturbances

INTECH
open science | open minds

InTech Europe
University Campus STeP Ri
Slavka Krautzeka 83/A
51000 Rijeka, Croatia
Phone: +385 (51) 770 447
Fax: +385 (51) 686 166
www.intechopen.com

InTech China
Unit 405, Office Block, Hotel Equatorial Shanghai
No.65, Yan An Road (West), Shanghai, 200040, China
中国上海市延安西路65号上海国际贵都大饭店办公楼405单元
Phone: +86-21-62489820
Fax: +86-21-62489821

IntechOpen